The Analysis of Parameter Sensitivity of Electron Backstreaming Failure Mode for 3-Grid System Ion Thruster

IEPC-2019-668

Presented at the 36th International Electric Propulsion Conference
University of Vienna • Vienna, Austria
September 15-20, 2019

JIA Yan-hui[1] and WANG Cong[2]
[1,2]*Science and Technology on Vacuum Technology and Physics Laboratory,*
Lanzhou Institute of Physics, Lanzhou 730000, China

Abstract: The key failure mode is electron backstreaming for 3-grid system ion thruster. The sensitive analysis result could guide to the ion thruster optimization design. The simulation model for electron backstreaming failure was developed by Hybrid-PIC-MCC method. The parameters were computed and compared for factors of screen gird voltage, accelerator grid voltage, the gap between screen and accelerator grid, plasma density upstream the screen gird in discharge chamber, and the propellant mass utilization efficiency in discharge chamber. The computed results indicated that the most sensitive parameter is the mass utilization efficiency in discharge chamber.

I.Introduction

THE ion electric propulsion system has the characteristics of high specific impulse, high efficiency, long service life and broad throttling. It can be used to perform spacecraft position keeping, orbit transfer, resistance compensation, attitude control and deep space explorer main propulsion mission [1]. The ion thruster is the heart of the ion-electric propulsion system, and is the key to the performance and longevity of the system. The failure of the grid system is a shortcoming of the performance and life of the ion thruster. To meet the long-life and multi-mode requirements of the all-electric propulsion and deep space exploration for the ion-electric propulsion system, the 5kW multi-mode LIPS-300 ion thruster that used 3-grid system was developed by LIP, in China. The 3-grid system adds a deceleration grid to the conventional 2-grid system. The deceleration grid can effectively improve the potential environment of the accelerator grid downstream, improve the extraction current of the gate beam, and reduce the sputter erosion of the downstream surface of the accelerator grid by exchanged charge ions, and extend the service life of the grid system [2]. The research result shows that the key failure model of the 3-grid system is the electron backstreaming that caused by the exchange of charge ions (CEX) on the accelerator grid orifice wall. The research focuses on the mechanism and process of electron reversal failure for an ion thruster. And the definition of the end of life, or the difference in precision of different algorithms for failure process simulation [3-8], did not systematically study the influence sensitivity of the relevant factors affecting the 3-grid system electron backstreaming failure model. The JPL has tested the sensitivity of NSTAR ion thruster anode flow rate, cathode flow rate and neutralizer flow rate to thruster discharge voltage and beam ion current [9], but has not focused on the impact on failure models.

In this paper, a Hybrid-PIC/MCC simulation model is developed to simulate the beamlet extraction,CEX ion generation and sputtering erosion of the 3-grid system. The simulated results can be reference to long life optimization design of the thruster.

---

[1]Senior engineer, Electric propulsion department, jiayh510@163.com.
[2]Master student, Electric propulsion department, wangc510@126.com.

II.The Simulation Model

A. The Mechanism of Electron Backstreaming Phenomenon

The electron backstreaming failure model is caused by the CEX ion bombardment sputtering of the accelerating grid orifice barrel, which causes the accelerator grid orifice to expand continuously. The acceleration grid orifice diameter increases, so that the absolute value of the negative electric saddle point voltage in the axial of the accelerator grid orifice is continuously reduced [10], as shown in Fig.1. It is shown that when the saddle point voltage is lowered below neutralization electron potential, it will not be able to prevent electrons from neutralization to the high potential discharge chamber and the screen grid region, and the grid system electron backstreaming failure model occurs. In Fig. 1, BOL represents the early life, EOL represents the end of life, lg represents the grid spacing, rs and ra represents the screen and the acceleration grid radius, respectively.

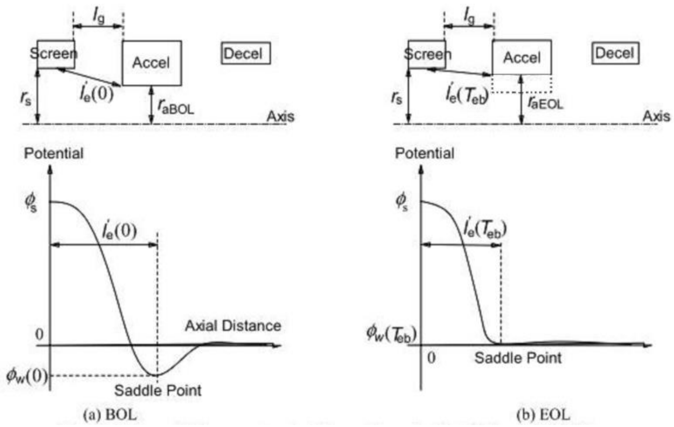

Fig 1 The grid shapes and potentials on the axis of gird apertures [6] (left: electrons backstreaming not appear, right: electrons backstreaming not appear)

B. The Simulation Region and Boundary Conditions

The three-dimensional problem of beam current extraction can be studied by a two-dimensional axisymmetric model, since of the grid orifice has axisymmetric characteristics. The 3-grid system simulated region and boundary conditions, as shown in Fig.2. That Z and R are the simulated region axial and radial lengths, respectively, and tsc is the screen thickness. tac is the thickness of the accelerator gird, tde is the thickness of the decelerator grid, d is the grid gap, rsc is the screen orifice radius, rac is the accelerator grid orifice radius, rde is the decelerator grid orifice radius, Vp is the discharge chamber plasma potential, and Vsc is the screen grid potential. The potential, Vac is the accelerator grid, and Vde is the decelerator grid potential. Parameters that used in simulation are listed in Table 1.

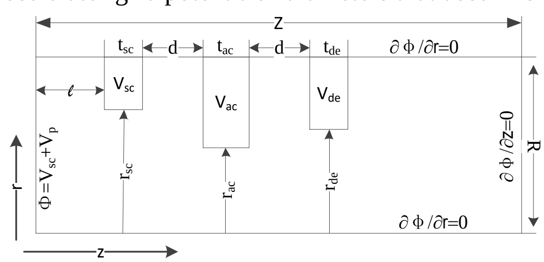

Fig.2 computation region and boundary

Table 1 The parameter of 3-grid system

Parameters	Value
Screen grid thickness/mm	0.40
Accelerator grid thickness/mm	0.50
Decelerator grid thickness/mm	0.40
Screen grid orifice radius/mm	1.90
Accelerator grid orifice radius/mm	1.25
Decelerator grid orifice radius/mm	1.60
Screen grid potential/V	1200

Accelerator grid potential/V	-400
Decelerator grid potential/V	0
Screen to accelerator grid gap/mm	1.00
Accelerator to decelerator grid gap/mm	1.00

When calculated the potential of the simulation region, the grid body is a constant potential that was set at beginning, the upstream edge is first boundary, and the rest is second boundary. When simulated the particle position, the left and right boundaries of the calculation region are absorption boundaries, and the rest are reflection boundaries.

C. Hybrid-PIC/MCC Model

Hybrid-PIC (Hybrid Particle in Cell) method is a commonly used numerical calculation method for studying the plasma transport characteristics of ion thrusters. Ions were treated as particles, and electron are treated as fluent. The collisions process is characters by Monte Carlo Collision (MCC). The simulation process of PIC/MCC is shown in Fig.3.

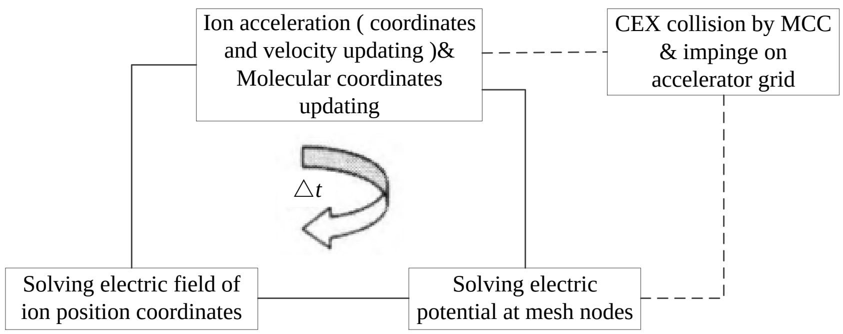

Fig.3 Flow scheme of PIC / MCC

The Poisson equation is used to solve the potential distribution of the simulation region, and the electric field at the location of the ions is solved by interpolation [10]. The motion of the ions follows the Newtonian equation, see equation (1). In the PIC model, the ions position and velocity are recorded and stored using a data link.

$$M\frac{dv}{dt}=E \qquad \frac{dx}{t}=v \tag{1}$$

Where Xe atomic mass, $2.18\times10^{-25}kg$; e is the unit charge, $1.60\times10^{-19}C$; $\boldsymbol{v}$ and $\boldsymbol{x}$ respectively are the velocity and position vector of the ion; $\boldsymbol{E}$ is the electric field strength at the location of the ion.

It is assumed that the Xenon atomic velocity follows the Maxwell distribution, enters the computational region from the upstream boundary at thermal velocity, and updates the position and velocity according to the defined time step length.

It is assumed that electrons density is subject the Boltzmann distribution, see equation (2),

$$n_e=n_{e,ref}\exp\left(\frac{\phi-\phi_{ref}}{T_{e,ref}}\right) \tag{2}$$

Where, n_e is the electron number density, ϕ is the potential, $n_{e,ref}$, $T_{e,ref}$ and ϕ_{ref} , respectively, the electron density, electron temperature, and the reference potential. When computed the electron density of the upstream and downstream of the accelerator grid, the reference point is the anode discharge and the downstream plume neutralization surface [5].

In the simulation model, the MCC mode is used to describe the exchange charge collision process between Xenon ions and Xenon atoms (including the residual Xenon atoms in the vacuum chamber and the Xenon atoms of didn't ionic that leaked from the grid orifice). The collision process can be expressed as Equation (3),

$$Xe^{+}_{fast}+Xe_{slow}\rightarrow Xe_{fast}+Xe^{+}_{slow} \tag{3}$$

Within a time step length, the collision probability of Xenon atoms and Xenon ions can be expressed as equation (4).

$$P_i=1-\exp(-\sigma(v_i)n(x_i)v_i\Delta t) \tag{4}$$

Where, x_i is the spatial position coordinate of the i-th ion; v_i is the velocity vector of the i-th ion; σ is the CEX collision cross section area, $\sigma = (k_1 \ln \Delta v + k_2)^2 \times 10^{-20}$, k_1 and k_2 are the constant, Δv is the relative velocity of the ion and atom at which the collision occurred; n is the atom density that collision happened; Δt is for time step length.

III.Simulation Grid Potential

A. Screen Grid Potential

According to the Child-Langmuir equation [12], the ion beam extraction capability of the grid system is proportional to the 1.5 power of the screen voltage. Therefore, the change in the screen voltage stress changes the beam density, which would affect the density of the CEX charge and ultimately changes. The sputtering rate of the accelerating barrel was affect by the screen potential. Fig.5 is a calculated result of the relationship between the screen grid beamlet current and the screen grid potential. The data points in Fig.4 is fitted to show that it can be character by $y = ax^{3/2} + b$, $a = 8.7\times10^{-20}$, $b = -8.8\times10^{-16}$.In this case, it is similar with the Child-Langmuir equation.

Fig.5 is a simulation result of the relationship between the accelerator grid barrel mass loss rate by sputtering. Fig.5 shows that it is 5.4 times at 2000V with 800v screen grid potential, and 2.6 times than 1200 V that designed screen grid of LIPS-300 ion thruster.

Therefore, the screen potential is one of the main design factors that affect the sputtering of accelerator grid orifice wall.

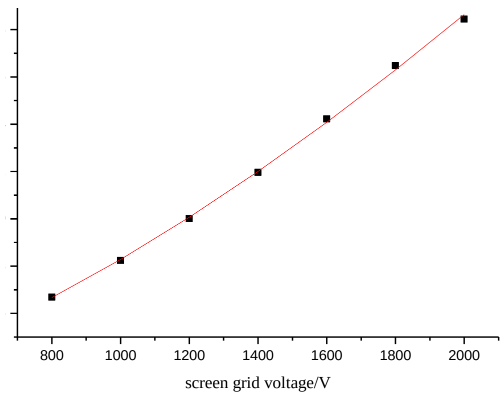

Fig.4 simulated result of beamlet current changing with the screen grid

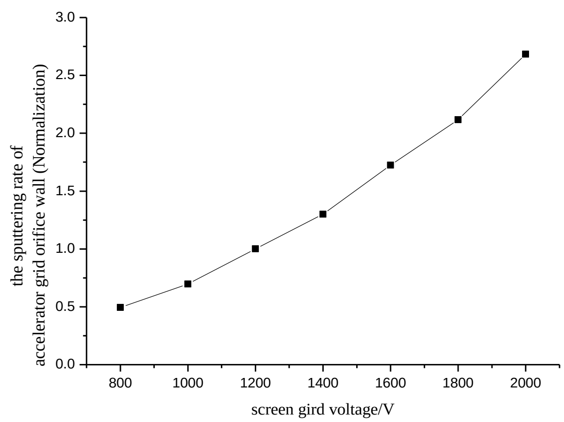

Fig.5 The changing of accelerator grid orifice wall sputtering rate along with the screen grid voltage

B. Accelerator Grid System

The most important reason for the sputtering of the acceleration grid structure material in the 3-grid system is the attraction of the acceleration grid negative potential to the slow CEX ions. Fig. 6 is a graph showing that the results of the sputtering rate of the accelerating gate orifice wall when the screen voltage is changed by the model. When the

CEX Xenon ion bombarded on the surface of the molybdenum grid is less than 1000 eV, the following mathematical relationship is approximated [13].

$$Y_0 = ax^2 + bx + c \tag{13}$$

Where, Y_0 is the sputtering yield, x is bombardment energy , and $a = -7.297 \times 10^{-7}$, $b = 2.515 \times 10^{-3}$, $c = -0.1866$.

It can be seen that when there is no order of magnitude change in the range of the acceleration grid voltage, the 3/2 times in the above equation can be neglected, and the sputtering yield of the grid material is proportional to the acceleration gate voltage, and the accelerator grid orifice wall shown in Fig.6. The relationship between the sputtering mass loss rate and the acceleration grid potential is in good agreement. According to Fig.6, with the LIPS-300 ion thruster accelerator grid potential -400V as the reference, when the absolute value of the acceleration grid potential is increased by 75% (-700V), the accelerator grid barrel sputtering rate is increased by 50%.

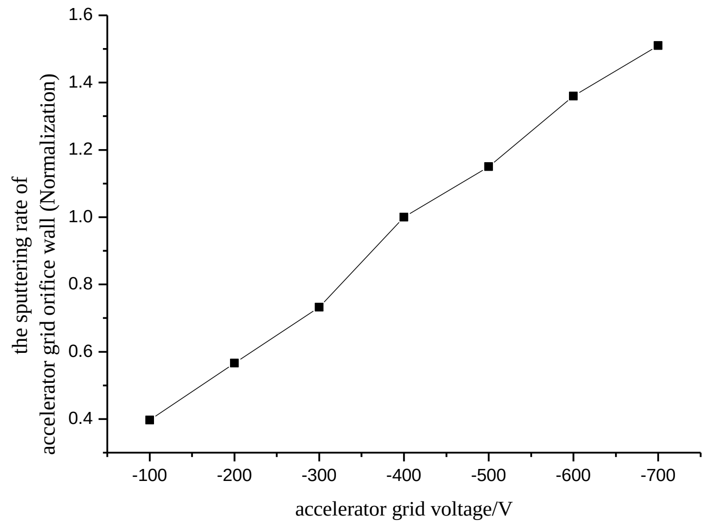

Fig.6 The accelerator grid orifice wall sputtering rate with different accelerator grid

C. The Gap That Between the Screen Grid and Accelerator Grid

As the gap between the screen grid and the accelerator grid is reduced, the ion beam is increased. According to the Child-Langmuir equation, the ion beam that extract from the grid system is 2 times with the gap of screen and accelerator grid. Therefore, when the other parameters are constant, the gap between the screen and accelerator grid is reduced, the value of the ion beam in the single orifice of the grid system is increased, and the probability that the beam ions collision with the atoms to generate CEX ions increases, which will accelerates the accelerator grid orifice sputtering mass lost. Fig. 7 is a calculation result of the mass loss rate by the sputtering of accelerator grid. The designed gap between screen and accelerator gird is 1.0mm. The calculation results in Fig.8 show that when the gap is reduced to 0.7mm, the sputtering rate of the accelerating grid orifice wall is increased by less than 10%. When the gap is increased to 1.3 mm, the sputtering rate is reduced by 21%.

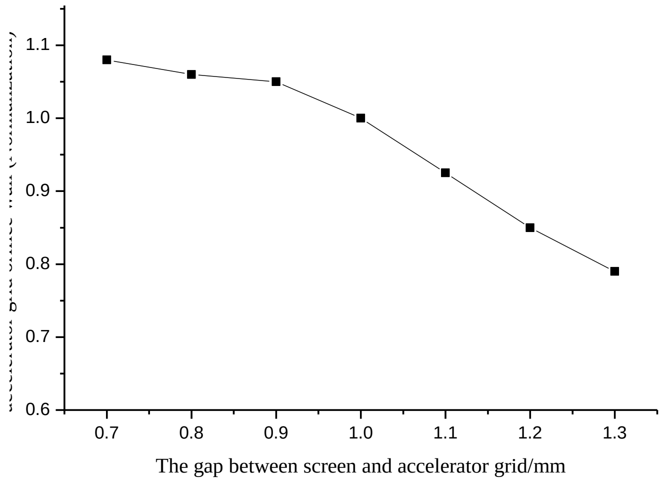

Fig.7 The accelerator grid orifice wall sputtering rate with different gap between the screen and accelerator grid

D. The Plasma Density in Discharge Chamber

According to the Child-Langmuir sheath theory of plasma, when the other design and working parameters are fixed, the ion beam is proportional to the plasma density in the discharge chamber where at the region of upstream of the screen grid, but it is limited by the effect of space charge limitation. The plasma density upstream of the screen grid exceeds the beam current extraction capability of the grid system, and under-perveance occurs. When the extraction ability of the grid system is much larger than the plasma density upstream of the screen, the over--perveance will occur. The simulation results of ion beam in different discharge chamber plasma density are shown in Fig8.

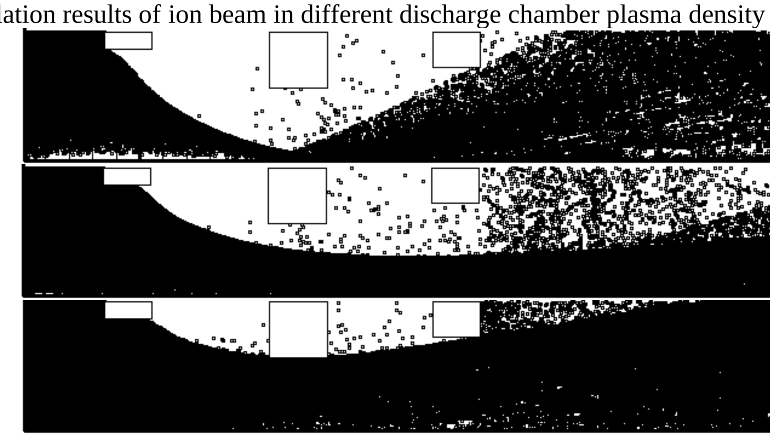

Fig.8 The beamlet ions and CEX distribution on under-, optimal-, and over-perveance for LIPS-300 ion thruster（plasma density upstream the screen grid in discharge chamber：up， $1.0\times10^{17}m^3$; **mid，** $4.0\times10^{17}m^3$ **；down，** $9.0\times10^{17}m^3$)

Fig.9 is ion beam current intercepted by the acceleration grid and the decelerator grid at different plasma density upstream of the screen. Fig.9 shows that the ion beam current is optimal-perveance in the plasma density range upstream of the appropriate screen, and there is no direct main beam ion interception in the acceleration grid and the deceleration grid. When the plasma density is lower, firstly the deceleration grating beam interception occurs, and the corresponding phenomenon is the over-perveance situation in Fig.8, when the plasma density is higher, the accelerator grid and the deceleration grid will exhibit intercept current, corresponding to the under-perveance condition in Fig8.

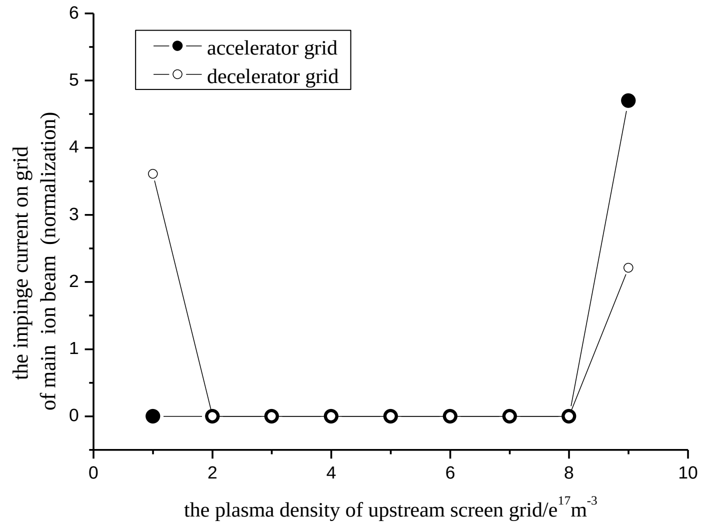

Fig. 9 the impinge current on different plasma density of upstream screen gird

Fig.10 is a simulated result of the sputtering mass loss rate of CEX ions to the accelerator grid orifice wall when the plasma density of the discharge chamber where is between $2\times10^{17}m^{-3}$ to $8\times10^{17}m^{-3}$. Fig.10 shows that the sputtering loss rate of the accelerating grid orifice is approximately linear with the plasma density of the screen upstream. When the plasma density of the screen upstream is doubled from the design value, the accelerator grid wall is sputtered. The sputtering rate has increased by a factor of 1.8.

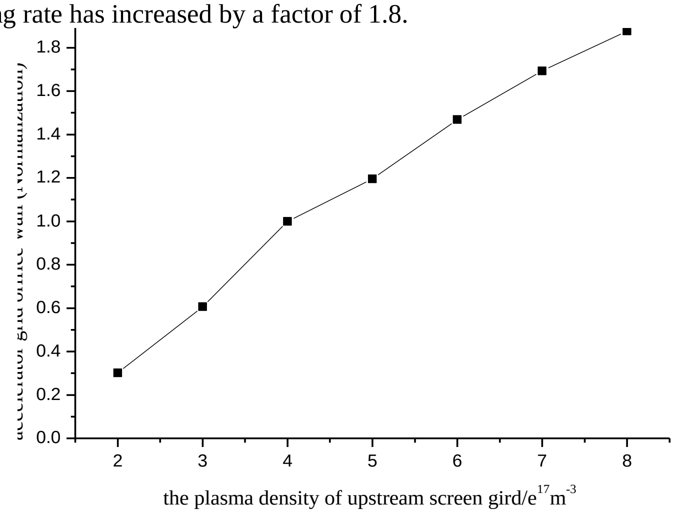

Fig.10 The accelerator grid orifice wall sputtering rate with different plasma density of upstream screen gird

E. The Propellant Mass Utilization Efficiency in Discharge Chamber

The propellant mass utilization efficiency is directly affecting the amount of Xenon atom number that escapes through the grid orifice. As the propellant mass utilization efficiency is decreased, the production rate of CEX ions increases accordingly. The influence mechanism is similar to the pressure stress of the vacuum chamber. Fig.11 is the accelerator grid orifice wall sputtering rate in different mass utilization efficiency. Fig.12 shows that when the propellant mass utilization efficiency in the discharge chamber is reduced from 90% to 60%, the sputtering loss rate of the accelerator grid orifice wall is increased by 4.0 times.

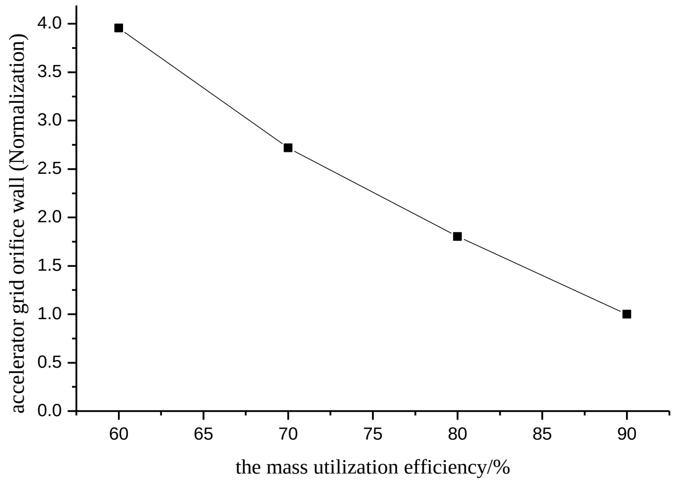

Fig.11 The accelerator grid orifice wall sputtering rate with different mass utilization efficiency

F. Comparative Analysis of Sensitivity Parameters

According to the above analysis, the propellant mass utilization efficiency is the most sensitivity parameter that caused electron backstreaming failure model, as it is listed in Fig.13, and the is the screen potential, the plasma density of the screen upstream, the accelerator grid potential, and the screen-acceleration grid gap.

As Fig.12 shows that after the performance index of the3-grid system ion thruster is determined, the long-life design should focus on propellant mass utilization efficiency in discharge chamber, but considering the comprehensive performance design of the thruster must also be comprehensive consideration in the discharge chamber mass utilization efficiency and discharge cost.

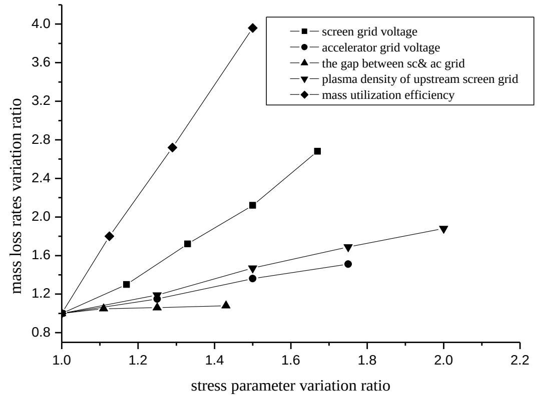

Fig.11 Comparison of sensitivity of accelerator grid orifice wall sputtering loss rate to different parameters

IV.Conclusion

In this paper, the simulation model is used to compute and analyze the sensitivity of different influencing factors of ion thruster electron backstreaming failure model caused by accelerator grid orifice wall sputtering of 3-grid system. The main conclusions are as follows:

(1) In the structure and working parameters of the grid system, the propellant mass utilization efficiency in discharge chamber is the most sensitive parameter that caused the electron backstreaming phenomenon of the 3-grid system ion thruster;

(2) According to the sensitivity parameter, the other parameters are the screen potential, the plasma density of the screen upstream, the accelerator grid potential and the screen-acceleration grid gap.

The calculation results can be used as a data reference for the parameter optimization in the long-life design.

Acknowledgments

JIA Yanhui thanks the support from the National Natural Science Foundation of China (11702123, 61601210), the Science and Technology Program of Gansu (18JR3RA412) and the Defense Industrial Technology Development Program (JSZL2017203B008).

References

[1]Hu J, Wang L, Zhang T.P. "Study on the equivalent magnetic circuit of ring magnetic field of LIPS-300 ion thruster," *Propulsion Technology*, 2018, 39(3): 713-720.

[2]Jia Y, Chen J, Guo N, et al. "2D Hybrid-PIC Simulation of the Two and Three-grid System of Ion thruster," *Plasma science and Technology*. 2018,12(2):240-247.

[3]Takeshi M, Katsuo "A. Effects of Electron Model on Three-Grid Ion Engine Analyses. IEPC-2011-205

[4]Sun A, Mao G, Yang J, et al. Particle Simulation of Three-Grid ECR Ion Thruster Optics and Erosion Prediction. *Plasma Science and Technology*.

[5]Chen Maolin, Xia Guangqing, Yang Zhengyan, et al. 3-D PIC Simulation of Ion Thruster Tri-Gate System. *High Voltage Engineering*,2014,40(10):3012-3017 .

[6]Masakatsu N. A Grid Lifetime Model for a 3-Grid Ion Engine," IEPC-2001-84.

[7]Tartz M, Hartmann E, Deltschew R, et al. "Grid Erosion Study of a Three-Grid Ion Thruster," AIAA 1998-3646

[8]Zhang Q, Peng X, Keefer D. "Particle Simulation of Grid Erosion for a Three-Grid Ion Thruster," IEPC 1993-178

[9]Sengupta A., Anderson J., Brophy John. "Sensitivity Testing of the NSTAR Ion Thruster," IEPC-2007-10

[10]Jia Yanhui, Zhang Tianping, Zheng Maofan, et al. "Numerical Analysis of the Electronic Backflow Threshold of the Ion Thruster Gate System," *Journal of Propulsion Technology*, 2012,33(6):991-996.

[11]Samantaroy R I, Hastings D E. "Particle-in-cell and monte carlo modeling of advanced plasma thrusters," SAO/NASA ADS,1995.

[12]Goebel D M, Katz I. "Fundamentals of Electric Prolusion: Ion and Hall Thruster," New Jersey,USA:John Wiley&Sons Inc.,2008:194-194.

[13]Brophy J R, Katz I, Plok J E, "Anderson J R. Numerical simulations of ion thruster accelerator grid erosion," AIAA-2002-4261.